J. Membrane Biol. 165, 77–90 (1998)

The Journal of
Membrane
Biology

The Barrier Domain for Solute Permeation Varies With Lipid Bilayer Phase Structure

T.-X. Xiang, Y.-H. Xu, B.D. Anderson
Department of Pharmaceutics & Pharmaceutical Chemistry, University of Utah, Salt Lake City, UT 84112, USA

Received: 16 September 1997/Revised: 14 May 1998

Abstract. The chemical selectivities of the transport barriers in lipid bilayers varying in composition and phase structure (gel-phase DPPC and DHPC bilayers and liquid-crystalline DPPC/CHOL/50:50 mol% bilayers) have been investigated by determining functional group contributions to transport of a series of α-substituted *p*-toluic acid analogs obtained in vesicle efflux experiments. Linear free energy relationships are established between the free energies of transfer for this series of compounds from water to the barrier domain and corresponding values for their transfer from water into six model bulk solvents (hexadecane, hexadecene, decadiene, chlorobutane, butyl ether, and octanol) determined in partitioning experiments to compare the barrier microenvironment to that in these model solvents. The barrier microenvironment in all bilayers studied is substantially more hydrophobic than octanol, thus establishing the location of the barrier beyond the hydrated headgroup interfacial region, as the interface is expected to be more hydrophilic than octanol. The chemical nature of the barrier domain microenvironment varies with bilayer phase structure. The barrier regions in non-interdigitated DPPC and interdigitated DHPC gel-phase bilayers exhibit some degree of hydrogen-bond acceptor capacity as may occur if these domains lie in the vicinity of the ester/ether linkages between the headgroups and the acyl chains. Intercalation of 50 mol% cholesterol into DPPC bilayers, which induces a phase transition to a liquid-crystalline phase, substantially increases the apparent barrier domain hydrophobicity relative to gel-phase bilayers to a nonhydrogen bonding, hydrocarbonlike environment resembling hexadecene. This result, combined with similar observations in liquid-crystalline egg-PC bilayers (*J. Pharm. Sci.* (1994), **83:**1511–1518), supports the notion that the transition from the gel-phase to liquid-crystalline phase shifts the barrier domain further into the bilayer interior (i.e., deeper within the ordered chain region).

Key words: Permeability — Partition coefficients — Lipid bilayers — Group contributions — Linear free energy relationships

Introduction

Biological membranes are described on a molecular level as fluid mosaics of proteins embedded within a lipid bilayer matrix (Singer & Nicholson, 1972). One of the major functions of biological membranes is to regulate the permeation of various chemical species into and out of cells. Although the transport of a large number of molecules of biological interest involves carriers and channel proteins, passive permeation across lipid bilayers occurs invariably for any chemical species driven by a gradient of the chemical potential and is the predominant mechanism by which most drug molecules reach their intended site of action.

One of the central and as yet unresolved issues in developing structure-activity relationships for various biological processes and in designing effective drugs and drug delivery systems is the determination of the locations and physicochemical nature of barrier domains in biological membranes for the transport of various molecular agents. Even in the absence of membrane proteins, uncertainty as to the location of the barrier domain arises due to the heterogeneity of *trans*-bilayer atomic distributions, reflecting (i) a hydrated headgroup interface, (ii) the ester/ether linkages between the headgroups and acyl chains, (iii) an ordered acyl chain region, and (iv) a region of relatively disordered acyl chains near the bilayer center. This heterogeneity is known to underlie the bell-shaped polarity profile (Griffith, Dehlinger & Van, 1974; Subczynski et al., 1994) within a bilayer interior as demonstrated in Fig. 1. In the absence of

Correspondence to: B. Anderson

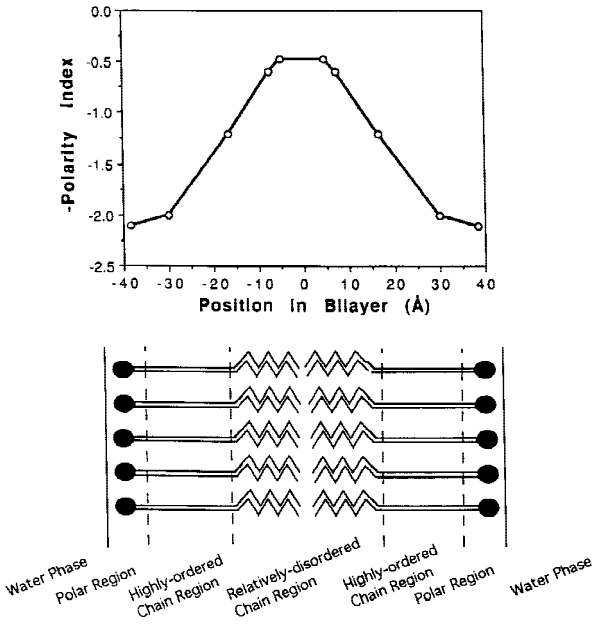

Fig. 1. The polarity (or hydrophobicity) profile in a microsomal lipid bilayer from calf liver as derived from spin-label ESR experiments. The definition of the polarity index and the experimental procedure for its acquisition were described by Griffith et al. (1974). These data serve only to demonstrate the nonuniformity of the chemical microenvironment within a particular lipid membrane. The actual polarity profiles in other lipid bilayers such as those investigated in this work may be significantly different. Furthermore, the effects of polar probes used on local polarity are not known.

chain ordering effects, the least polar region would impose the highest energetic barrier to the transport of polar permeants. However, chain ordering in bilayers imposes an additional diffusional resistance and an entropic barrier to partitioning, respectively (Bassolino-Klimas, Alper & Stouch, 1993; Marqusee & Dill, 1986; Xiang & Anderson, 1995*a*), such that the actual location of the transport barrier domain is determined by the balance of these factors.

The degree of success achieved using Hansch π parameters, obtained from octanol/water partition coefficients (Leo, Hansch & Elkins, 1971), in correlating transport processes in biological membranes supports Overton's suggestion that solute permeability through biological membranes correlates with the corresponding bulk oil/water partition coefficient (Overton, 1899). However, membranes with different lipid composition may display substantially different chemical selectivity to solute transport. For example, studies in the authors' laboratories using functional group contributions have shown that the barrier domain for transport across human stratum corneum, the barrier properties of which are generally attributed to the multiple lamellae of lipid bilayer membranes localized within its intercellular spaces, closely resembles octanol in its selectivity to permeant structure (Anderson, Higuchi & Raykar, 1988; Anderson & Raykar, 1989). Similarly, correlations between octanol/water partition coefficients and transport of solutes across the blood-brain barrier are well established (Levin, 1980; Rapoport, Ohno & Pettigrew, 1979). On the other hand, recent studies in egg lecithin bilayers, also conducted in the authors' laboratories, have demonstrated a chemical selectivity for this membrane more closely resembling that expected if the barrier domain were hydrocarbonlike, with negligible hydrogen bonding capacity (Xiang & Anderson, 1994; Xiang, Chen & Anderson, 1992).

To maintain certain biological functions, many natural membranes exist in a highly ordered state either through changes in phase structure or through intercalation of various ordering agents such as cholesterol and sphingomyelin (van Blitterswijk, van der Meer & Hilkmann, 1987). For example, some natural plasma membranes contain up to a 50% mole fraction of cholesterol. Key lipid constituents isolated from the intercellular lipid bilayers in the outer layer of the skin (viz., the stratum corneum) (Lampe, Williams & Elias, 1983; White, Mirejovsky & King, 1988) and from brain myelin (Clowes, Cherry & Chapman, 1971) exist mainly in a gel phase or a gel-fluid phase coexistence region at physiological temperatures. Although increases in bilayer chain ordering are known to systematically reduce solute permeabilities (Xiang & Anderson, 1995*b*; Xiang & Anderson, 1997), how these changes alter the *chemical* selectivity of lipid bilayers to solutes varying in polarity and in the number and nature of hydrogen bonding substituents remains unclear.

Some evidence also suggests that the carbonyl dipoles present in most phospholipids have an important influence on the polarity within the bilayer interior (Flewelling & Hubbell, 1986). However, the effect of the mode(s) of linkage of the hydrocarbon chains to the glycerol moiety in phospholipids on barrier properties has not yet been addressed. Although the linkage is through an ester bond in most phospholipids of biological interest, ether bonded lipids exist in mammalian membranes and other biological membranes and the functional potency of certain lipids is attributed to this ether linkage (Snyder, 1985). Thus, a comparative study of the effects of ester and ether linkages on the chemical selectivity of the barrier domain in phospholipid bilayers would shed light on changes of local polarity as a result of these linkage alterations.

This study examines the permeability coefficients for a series of α-substituted *p*-toluic acid analogues in LUVs composed of dipalmitoylphosphatidylcholine (DPPC), dihexadecylphosphatidylcholine (DHPC) and DPPC/Cholesterol (CHOL) (50:50 mol%). The permeability coefficients (P_m) obtained and the incremental free energies of transfer from water to the barrier domain

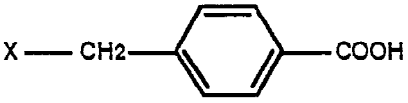

a - g

SUBSTRATE	X
a	-H
b	-Cl
c	-OCH_3
d	-CN
e	-OH
f	-COOH
g	-$CONH_2$

Fig. 2. Molecular structures of α-substituted *p*-toluic acids employed in this study.

for individual functional groups calculated from these P_m values are compared with corresponding values from partition coefficient measurements between water and 1-octanol, butyl ether, 1-chlorobutane, 1,9-decadiene, 1-hexadecene, and n-hexadecane, respectively. Previous transport studies to obtain functional group contributions were performed in these laboratories using ''black'' lipid membranes (BLM) containing egg lecithin (Xiang & Anderson, 1994; Xiang et al., 1992). Because of the difficulty of forming stable ''black'' lipid films using saturated phospholipids and uncertainty as to the true lipid compositions in ''black'' lipid bilayers composed of more than one lipid component, a vesicular efflux method was developed using large unilamellar vesicles in conjunction with size-exclusion chromatography and ultrafiltration. This transport method overcomes the shortcomings inherent in BLM experiments and allows flux to be monitored over a longer time frame than other methods. The series of α-substituted *p*-toluic acids were chosen as their polar substituents are sufficiently isolated to preclude the possibility of intramolecular hydrogen bonding with other substituents in the same molecule. The presence of an ionizable -COOH group allowed permeability coefficients varying over roughly 5–6 orders of magnitude to be determined by selecting a suitable pH ''window'' for each permeant so that fluxes were in a detectable range.

Materials and Methods

Chemicals

DPPC (>99%), DPPA (>99%), and egg-lecithin (>99%) were purchased from Avanti Polar Lipids, (Pelham, AL). DHPC (99%), cholesterol (99+%) and ^{3}H-cholesterol (1 mCi/mL) were purchased from Sigma Chemical (St. Louis, MO). All lipids were stored in a freezer upon arrival. Chlorobutane (99.5%) and butyl ether (99.3%) were obtained from Aldrich Chemical (Milwaukee, WI). ^{3}H-D-glucose (1 mCi/mL, specific activity = 60 Ci/mmol) and ^{3}H-mannitol (1 mCi/mL, specific activity = 15 Ci/mmol) were obtained from American Radiolabeled Chemicals (St. Louis, MO). The structures of the α-substituted *p*-toluic acids used as permeants in the transport experiments are shown in Fig. 2. *p*-Toluic acid (>98%, Sigma), α-hydroxy-*p*-toluic acid (Sigma) and α-chloro-*p*-toluic acid (95%, Aldrich) were used as received without further purification. The remaining compounds in Fig. 2 were synthesized as reported previously (Xiang & Anderson, 1994). Final purities of all compounds synthesized were >95% by HPLC.

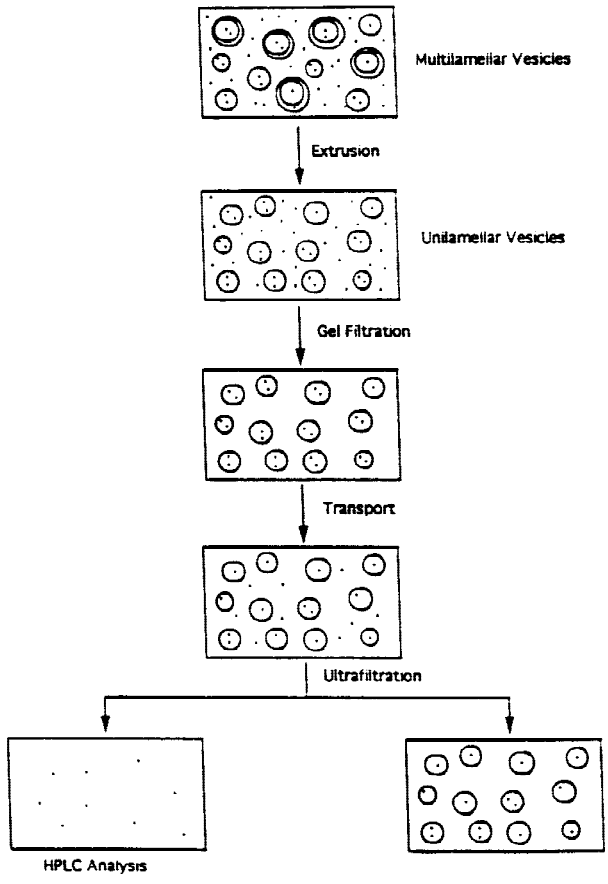

Fig. 3. Flow diagram of the experimental procedures employed for determining permeability coefficients.

Determination of Permeability Coefficients

Permeant efflux from LUVs was monitored to obtain lipid bilayer permeability coefficients. The experimental procedure, as depicted by a flow chart in Fig. 3, included the steps described below.

LUV Preparation and Characterization

Lipids were accurately weighted, dissolved in chloroform, evaporated to a dry thin film on the bottom of a round-bottom flask, and left under

vacuum for 2 hr at ≈50°C. An aqueous solution containing (1–3) × 10^{-3} M *p*-toluic acid analogue (cold compound) or 10 μ Ci/mL radiolabeled α-D-glucose, 0.04 M buffer (MES, phosphate or carbonate) at a given pH and ionic strength (0.1, adjusted with sodium chloride) was then added to a final total lipid concentration of 5–7.5 mg/mL. The lipids were hydrated by repeated vortexing and shaking at ~50°C, well above the main transition temperatures for DPPC (41°C) or DHPC (44°C). The lipid suspensions formed were then forced through 0.2 μm polycarbonate filters (Nuclepore, Pleasanton, CA) 17 times at ~50°C to form LUVs. A small amount of dipalmitoylphosphatidic acid (DPPA, 4 mol %) was added to these lipid systems to prevent aggregation and increase LUV stability (Cevc et al., 1988). This small amount of DPPA has been shown to have a minimal effect on bilayer phase structure (Marra-Feil, 1995).

Vesicle hydrodynamic diameters, *d*, were determined by dynamic light scattering (DLS) measurements on every vesicle preparation. The apparatus for DLS experiments consisted of a goniometer/auto correlator (Model BI-2030AT, Brookhaven, Holtsville, NY) and an Ar^+ ion laser (M95, Cooper Laser Sonics, Palo Alto, CA) operated at 514.5 nm wavelength. One drop of LUV suspension was placed in a clean glass test tube (13 × 75 mm) and brought to a volume of 2 mL with the same filtered buffer solution. The sample was placed in a temperature-controlled cuvette holder with a toluene index-matching bath. Autocorrelation functions were determined for a period of 100 sec with a 10–80 μsec duration at 90° and analyzed by the method of cumulants.

The captured liposomal volume was measured in a single batch (3 samples) according to a method developed by Hope et al. (1985). The liposomes were prepared in the presence of 5 μCi/ml mannitol. An aliquot (60 μl) was then loaded onto a Sephadex column and eluted by centrifugation (vida supra). This was sufficient to remove all the unentrapped material. Aliquots of the eluted sample were then assayed for phosphorus content and entrapped ^{3}H-mannitol.

To determine if the extrusion and gel filtration (described below) steps significantly altered the lipid composition of DPPC/CHOL (50:50 mol ratio) vesicles, the initial lipid preparations (a single batch of three samples) were spiked with radiolabeled cholesterol (2 μCi) and the contents of cholesterol and DPPC lipids in the samples before and after the extrusion and gel filtration were analyzed for ^{3}H-cholesterol and phosphorus (Bartlett, 1959).

Gel Filtration

Aliquots (0.5–0.6 ml) of the LUVs prepared above were loaded onto a size-exclusion column packed with Sephadex G-50 (medium fractionation range, Sigma) in a 10-ml disposable syringe and equilibrated at 25°C with the same buffer solution as that used to prepare the LUVs but without permeant. The permeant loaded LUV samples was then eluted by centrifugation (Model CL, IEC, Needham Hts., MA) at two-speeds (2 min at $g = 300$; 1 min at $g = 900$). The pH of the eluent was monitored to make sure that the eluent pH and that in the original LUV sample were identical. Vesicles with entrapped permeant appeared in the void volume of the size-exclusion column and were well separated from the fraction of extravesicular permeant. HPLC analyses of initial and equilibrium extravesicular permeant concentrations in the LUVs indicated an initial ratio of the entrapped to extravesicular permeant concentration after size-exclusion chromatography on the order of 10^5. The eluted LUVs were collected in a screw-capped 10-ml glass vial and immediately placed in a 25°C water bath.

Ultrafiltration

The concentration gradient created by gel filtration resulted in a net flux of permeant across the LUVs and a continuous increase in the permeant concentration outside the LUVs with time. To determine the flux, aliquots (0.4 ml) of the LUVs after the gel filtration were taken at various time intervals and loaded onto a Centricon-100 filter (MWCO = 100,000; Amicon, Beverly, MA). The loaded sample was then centrifuged at $g = 1{,}200$ for 3–6 min. The effects of permeant binding to the Centricon-100 filter on filtrate concentrations were examined with selected permeants and at several different permeant concentrations. No significant binding was detected after new filters were preconditioned by rinsing with deionized water. Permeant concentrations in the collected filtrate (*ca.* 100–200 μl) were subsequently analyzed by HPLC for α-substituted *p*-toluic acids or by liquid scintillation counting (Beckman LS1801, Beckman Instr., Fullerton, CA) for ^{3}H-glucose after 100 μl of the filtrate was mixed with 3 ml of a scintillation cocktail (Aquasol, Opti-Fluor, Packard Instrument, Meriden, CT). Total permeant concentrations in the LUVs were determined by lysing samples with a small amount of Triton X-100 (Sigma) prior to analysis.

HPLC Analyses

An HPLC system consisting of a syringe-loaded sample injector (Rheodyne Model 7125, Rainin Instrument, Woburn, MA), a solvent delivery system (110B, Beckman Instruments, San Ramon, CA) operated at a flow rate of 0.6–1.0 ml/min, a dual-wavelength absorbance detector (Model 441, Water Associates, Milford, MA) operated at 254 nm, an integrator (Model 3392A, Hewlett-Packard, Avondale, PA), and a reversed-phase column packed with 5 μm Spheri-5 RP-18 (Brownlee OD-MP, 4.6 mm i.d. × 10 cm, Rainin) was used at ambient temperature for the analyses of the samples taken during the transport and partition experiments. Acetonitrile:water mobile phases varying from 10 to 30% organic solvent depending on the analyte lipophilicity and buffered to a pH of 3.0 using 0.01 M phosphate buffer were employed.

Modeling of Flux Data

The entrapped permeant concentration varies with time according to the following kinetic equation

$$-\frac{dC_i^t}{dt} = k_{obs}(C_i^t - C_o^t) \tag{1}$$

where C_i^t and C_o^t are permeant concentrations inside and outside LUVs at time *t*, respectively, and k_{obs} is the first-order rate constant. Since the total mass of permeant in the sample is a constant and C_i is equal to C_o at equilibrium, one obtains

$$C_o^t = \frac{1}{V_o}[(V_i + V_o)C_o^\infty - V_i C_i^t] \tag{2}$$

where V_i and V_o are the total internal and external aqueous volumes, respectively. Combining Eqs. 1 and 2 and considering the fact that $V_i << V_o$, Eq. 1 becomes

$$\frac{dC_o^t}{dt} = k_{obs}(C_o^\infty - C_o^t) \tag{3}$$

Solving this differential equation with the known initial concentration, C_o^o, gives

$$ln(C_o^\infty - C_o^o)/(C_o^\infty - C_o^t) = k_{obs}t \quad (4)$$

The apparent permeability coefficient P_{app} can be obtained from the first-order rate constant, k_{obs}, and the ratio between the entrapped volume and surface area of the LUVs, V/A, via the equation

$$P_{app} = k_{obs}\, V/A_t \quad (5)$$

The V/A ratio is obtained from the vesicle hydrodynamic diameter, *d*, via the equation, $V/A = d/6$.

Determination of Partition Coefficients

The octanol/water, decadiene/water, hexadecene/water, and hexadecane/water partition coefficients for the series of *p*-toluic acid analogues were obtained previously (Xiang & Anderson, 1994). In this study, chlorobutane/water and butyl ether/water partition coefficients for the same series of compounds were determined using the same shake flask method as used previously. In brief, a 1-ml aqueous solution with $(0.2 - 1) \times 10^{-4}$ M permeant and 0.1-M NaCl was placed in a 5-ml test tube along with 1–2 ml of organic solvent. The sample was vortexed and centrifuged, then allowed to stand in a water bath at 25°C for 5 hr. Aliquots were carefully withdrawn from both phases for subsequent analysis by HPLC as described above. The aqueous phase was maintained at a pH >2 units below the permeant pK_a value(s) by titration with 0.1 N HCl. The organic solvents were washed three times with an equal volume of deionized water before the partition experiments.

Results and Discussion

Vesicle Characterization

The captured liposomal volume measured in DPPC vesicles according to a method developed by Hope et al. (1985) was found to be 3.3 ± 0.4 L/mol lipid. The average diameter of these vesicles as measured by dynamic light scattering was 160 ± 10 nm. Assuming a bilayer thickness of 4.46 nm and a surface area per lipid molecule of 0.48 nm^2 (Braganza & Worcester, 1986), the captured volume for a unilamellar dispersion of 160 nm vesicles should be 3.4 L/mol lipid, in close agreement with the experimental results. Using a similar method of preparation, Marra-Feil (1995) also demonstrated by freeze-fracture techniques that the vesicles formed are primarily unilamellar.

To determine if the extrusion and gel filtration steps significantly altered the lipid composition of DPPC/CHOL (50:50 mol ratio) vesicles, the initial lipid preparations were spiked with radiolabeled cholesterol (2 μCi) and the contents of cholesterol and DPPC lipids in the samples before and after the extrusion and gel filtration were analyzed. The cholesterol composition after the extrusion and gel filtration steps was 46 ± 5 mol%, equal to the expected 50 mol% cholesterol within experimental error.

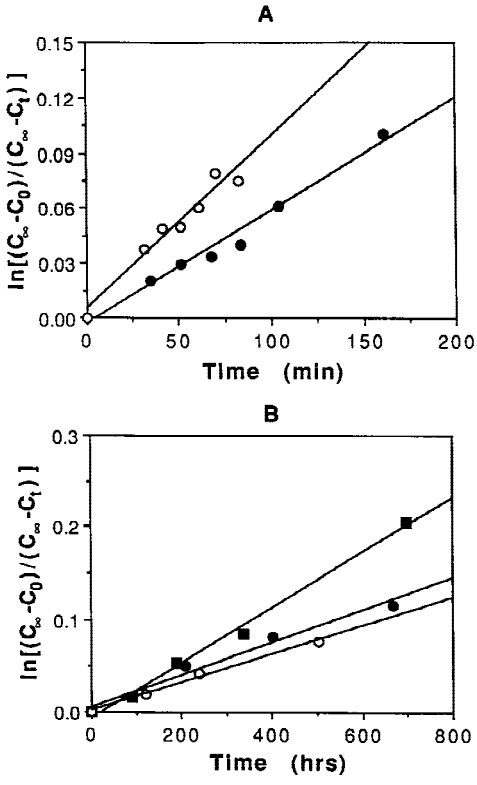

Fig. 4. Representative first-order release profiles *vs.* time for ^{3}H-α-D-glucose. (*A*) across egg-PC bilayers (●, extrusion through 0.2 μm filters; and ○, extrusion through 0.1 μ filters). (*B*) across DPPC (●), DHPC (○), and DPPC/CHOL (■) bilayers.

Bilayer Permeability Coefficients

To validate the transport methods employed in this study, the permeation rates for radiolabeled α-D-glucose across egg-lecithin vesicles were measured and compared to available literature values. Figure 4*A* shows two representative release profiles *vs.* time for α-D-glucose across egg-PC liposomes formed by extrusion through 0.1 or 0.2 micron polycarbonate filters. Rate constants, k_{obs}, were determined from the slopes of the lines representing linear least-squares fits of the data, from which the apparent permeability coefficients, P_{app}, were calculated according to Eq. 5 using vesicle hydrodynamic diameters obtained in DLS measurements to obtain *V/A* ratios. The glucose permeability coefficients obtained were $(2.7 \pm 0.4) \times 10^{-11}$ cm/sec and $(3.3 \pm 0.5) \times 10^{-11}$ cm/sec for egg-lecithin vesicles prepared by extrusion through 0.1 and 0.2 μm polycarbonate filters, respectively. These values are in close agreement with the results of Brunner et al. (1980), $(3 \pm 2) \times 10^{-11}$ cm/sec. Since a reduction of filter pore-size from 0.2 micron to 0.1 micron is expected to decrease the percentage of multilamellar vesicles (Hope et al., 1985), the absence of a significant difference between the permeability coefficients ob-

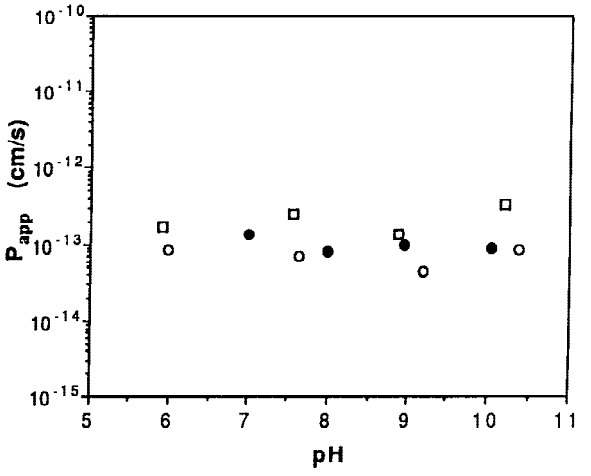

Fig. 5. Permeability coefficients versus pH for α-D-glucose across DHPC (○), DPPC (●) and DPPC/CHOL (□) bilayers.

tained in vesicles prepared by extrusion through 0.1 and 0.2 μm polycarbonate filters suggests that the small percentage of multilamellar vesicles likely to be present had only a minor influence on the permeability measurements.

Liposomes consisting of DPPC, DHPC, DPPC/CHOL (50:50 mole ratio) lipids were employed for this study. The phase structures for these lipid bilayers have been established from numerous recent studies using ^{13}C and ^{2}H-NMR, ESR and DSC methods (Huang et al., 1993; Ruocco, Siminovitch & Griffin, 1985; Sankaram & Thompson, 1991; Vist & Davis, 1990). These studies have clearly shown that at 25°C, DPPC and DHPC bilayers consist of single noninterdigitated and interdigitated gel phases, respectively, and DPPC:CHOL bilayers at a 1:1 mole ratio exist in a single ordered liquid-crystalline phase. Using an NMR line-broadening permeability method, we have shown that phase separations in DPPC:CHOL bilayers at 25°C occur only in a cholesterol concentration range between 0.05 and 0.3 mole fraction (Xiang & Anderson, 1998), much lower than the cholesterol concentration used in this study (0.5 mole fraction). Thus, all systems employed consisted of a single lipid phase.

The permeability coefficients for α-D-glucose across DPPC, DHPC, and DPPC/CHOL (50:50 molar ratio) were also determined over the pH range of interest to assess the dependence of barrier properties on pH. Since glucose is not ionizable within the pH range explored, any systematic change of P_{app} with pH would reflect an alteration of bilayer barrier properties with pH. Figure 4*B* shows three representative release profiles versus time for α-D-glucose across DPPC, DHPC, and DPPC/CHOL (50:50 mole ratio) liposomes. The permeability coefficients obtained are plotted in Fig. 5 as a function of solution pH. As noted, P_{app} for α-D-glucose is independent of pH, consistent with previous observations demonstrating the pH independence of the permeability of acetamide across egg-PC bilayers (Xiang et al., 1992). Particularly noteworthy is the finding that the permeability coefficients for α-D-glucose across the gel-phase DPPC and DHPC bilayers and the cholesterol-rich ordered DPPC bilayers (P_{app} = (0.4–3.3) × 10^{-13} cm/sec) are 2–3 orders of magnitude smaller than the P_{app} across the relatively disordered egg-PC bilayers, demonstrating the strong effects of bilayer chain ordering on solute transport.

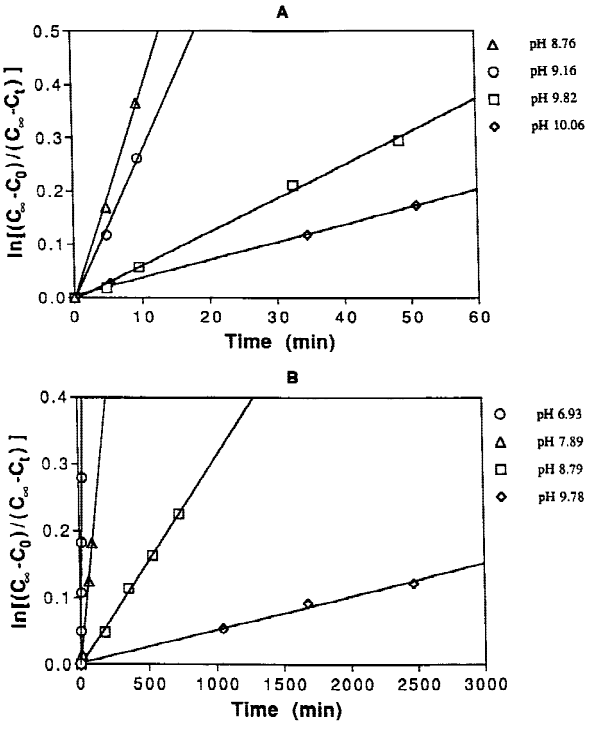

Fig. 6. Representative first-order release profiles versus time for *p*-toluic acid (*A*) and α-hydroxy-*p*-toluic acid (*B*) across DHPC bilayers at four different pH values.

Representative efflux measurements for *p*-toluic acid and α-hydroxy-*p*-toluic acid across DHPC bilayers at four different pH values are plotted in Fig. 6*A* and *B*, respectively, according to Eq. 4. The possible effects of permeant self-association in the bilayers on permeability were examined for a selected permeant (α-hydroxy-*p*-toluic acid) by varying the permeant concentration over 0.01–10 mM at pH = 8.0. No systematic change in the permeability coefficient was observed (*data not shown*). As illustrated in Fig. 6*A* and *B*, the rate constants for both *p*-toluic acid and α-hydroxy-*p*-toluic acid are strongly dependent on solution pH but at any given pH *p*-toluic acid has a much greater rate constant than α-hydroxy-*p*-toluic acid. Semilogarithmic P_{app} *vs.* pH profiles for the series of *p*-toluic acid analogues listed in Fig. 2 across gel-phase DPPC bilayers, interdigitated gel-phase DHPC

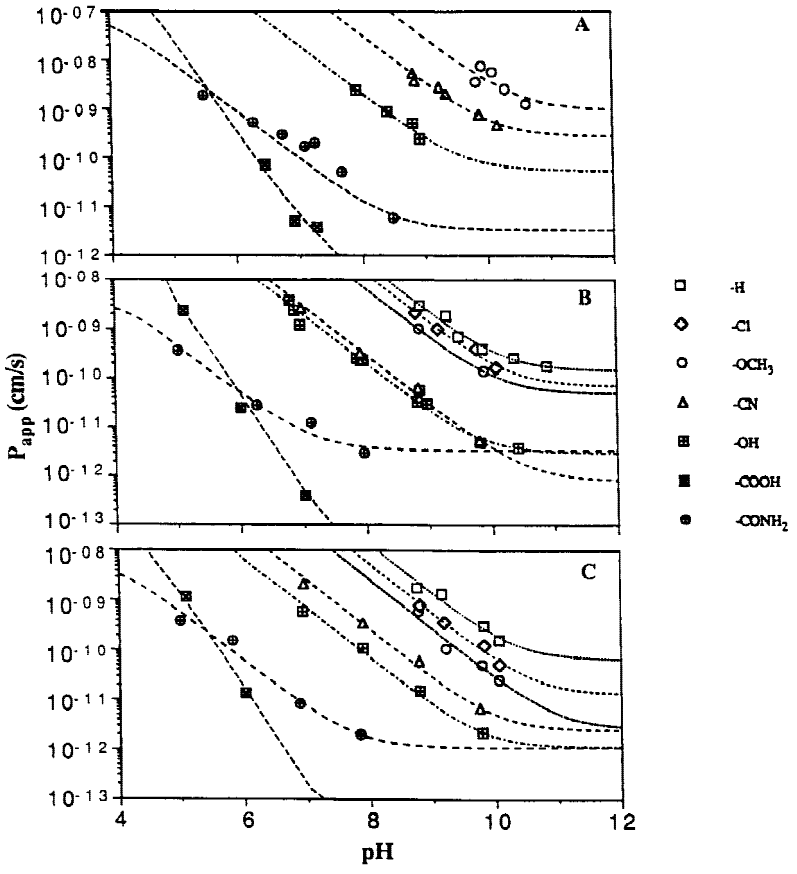

Fig. 7. Apparent permeability coefficients *vs.* pH for the series of *p*-toluic acid analogues across DPPC/CHOL (*A*), DPPC (*B*) and DHPC (*C*) bilayers. The curves were generated by nonlinear least-squares fits according to Eqs. 6–8.

bilayers and ordered liquid-crystalline phase DPPC/CHOL (50:50) bilayers are presented in Fig. 7*A–C*, respectively. (In DPPC/CHOL bilayers, the permeation rates for the most lipophilic permeants in the series, *p*-toluic acid and α-chloro-*p*-toluic acid, were too fast to be detected by the present method.)

At a given pH, these analogues exist partially in their neutral form (HA) and partially as anions (A^-), determined by their characteristic dissociation constants, K_a. Since the bilayer barrier properties are independent of pH and neutral and ionized permeants are known to exhibit considerably different permeability coefficients (Xiang et al., 1992), the variation of P_{app} with pH for these compounds shown in Fig. 7*A–C* may therefore be attributed to the different permeability coefficients of the neutral and anionic species, P^{HA} and P^A, respectively, and changes in the relative fractions of *HA* and A^- with solution pH. In the absence of unstirred layer effects (negligible in this study), the apparent permeability coefficient can be expressed as

$$P_{app} = f_{HA}P^{HA} + (1 - f_{HA})P^A \tag{6}$$

where the fraction of neutral species *HA* is

$$f_{HA} = \frac{1}{1 + K_a/[H^+]} \tag{7}$$

or

$$f_{HA} = \frac{1}{1 + K_{a1}/[H^+] + K_{a1}\,K_{a2}/[H^+]^2} \tag{8}$$

for a monocarboxylic acid or a dicarboxylic acid, respectively. Acid dissociation constants for the series of *p*-toluic acid analogues were determined previously (Xiang & Anderson, 1994). According to Eq. 6, at low pH where $[H^+] >> K_a$ (or K_{a1} and K_{a2} for α-carboxy-*p*-toluic acid), f_{HA} approaches one and P_{app} reaches a plateau value of P^{HA}. At high pH, f_{HA} becomes negligible and P_{app} approaches a limiting value of P^A. At intermediate pH values, where $[H^+] << K_a$ (or K_{a1} and K_{a2} for the dicarboxylic acid) but $f_{HA}P^{HA}$ is still much greater than $(1 - f_{HA})P^A$, $P_{app} \approx P^{HA}[H^+]/K_a$ ($P_{app} \approx P^{HA}\,[H^+]^2/K_{a1}K_{a2}$ for the dicarboxylic acid), and $\log P_{app}$ is linearly dependent on pH with a slope of −1 or −2. The curves shown in Fig. 7*A–C*, which represent nonlinear regression analyses of the data according to Eq. 6, indicate that this model can satisfactorily describe the P_{app} *vs.* pH profiles generated. The permeability coefficients for the neutral species of the *p*-toluic acid analogues across DHPC, DPPC and DPPC/CHOL bilayers obtained from the non-linear fits are summarized in Table 1 along with those in egg-PC bilayers determined previously in these

Table 1. Permeability coefficients (cm/sec) for neutral α-substituted *p*-toluic acid analogues across four different lipid bilayer membranes at 25°C[a]

Permeant	X	Lipid Bilayer Composition			
		DHPC	DPPC	DPPC/CHOL	Egg-PC[c]
a	−H	$(6.3 \pm 0.2) \times 10^{-5}$	$(1.3 \pm 0.2) \times 10^{-4}$	–[b]	1.1 ± 0.2
b	−Cl	$(4.9 \pm 0.4) \times 10^{-5}$	$(1.3 \pm 0.1) \times 10^{-4}$	–[b]	$(6.4 \pm 0.1) \times 10^{-1}$
c	$-OCH_3$	$(2.6 \pm 0.7) \times 10^{-5}$	5.8×10^{-5}	$(2.5 \pm 1.4) \times 10^{-3}$	$(3.5 \pm 0.1) \times 10^{-1}$
d	−CN	$(2.1 \pm 0.2) \times 10^{-6}$	$(2.6 \pm 0.1) \times 10^{-6}$	$(2.6 \pm 0.4) \times 10^{-4}$	$(2.7 \pm 0.5) \times 10^{-2}$
e	−OH	$(4.5 \pm 0.5) \times 10^{-7}$	$(1.4 \pm 0.2) \times 10^{-6}$	$(1.4 \pm 0.2) \times 10^{-5}$	$(1.6 \pm 0.4) \times 10^{-3}$
f	−COOH	$(1.6 \pm 0.1) \times 10^{-7}$	$(3.4 \pm 0.3) \times 10^{-7}$	$(4.0 \pm 0.6) \times 10^{-6}$	$(1.8 \pm 0.3) \times 10^{-4}$
g	$-CONH_2$	$(5.1 \pm 1.2) \times 10^{-9}$	$(4.6 \pm 0.3) \times 10^{-9}$	$(1.1 \pm 0.3) \times 10^{-7}$	$(4.1 \pm 0.4) \times 10^{-5}$

[a] Expressed as mean ± SD.
[b] Too fast to be detectable by the present method.
[c] Determined from previous experiments using the BLM transport method (Xiang & Anderson, 1994).

laboratories using the BLM method (Xiang & Anderson, 1994).

Barrier Domain Model for Lipid Bilayer Transport

The overall resistance of a heterogenous bilayer membrane to solute permeation, as expressed by the inverse of permeability coefficient P_m, is the summation of the resistances in different regions across the bilayer (Diamond, Szabo & Katz, 1974), or

$$\frac{1}{P_m} = \int_0^d \frac{dz}{K_{z/w} D_z} \tag{9}$$

where $K_{z/w}$ and D_z are the partition coefficient from water into and the diffusion coefficient in the bilayer at position z for the permeating solute, respectively, and d is the entire bilayer thickness including the bilayer/water interface. If transport is governed primarily by a distinct region within the lipid bilayer, however, it may be possible to describe the permeability coefficient, P_m, by the following solubility-diffusion model:

$$P_m = \frac{K_{barrier/w} D_{barrier}}{d_{barrier}} \tag{10}$$

where $K_{barrier/w}$ and $D_{barrier}$ are the partition coefficient from water into and the diffusion coefficient in the bilayer barrier domain for the permeating solute, respectively, and $d_{barrier}$ now represents the thickness of the barrier domain. Since the series of compounds listed in Fig. 2 are similar in molecular size and shape and therefore are likely to exhibit similar diffusional characteristics and volume displacement within lipid bilayers, their inherent polar/hydrogen bonding nature which determines $K_{barrier/w}$ becomes the predominant variable influencing their relative permeabilities. However, macroscopic membrane/water partition coefficients which are experimentally accessible may not be a good measure of the relevant partition coefficients, $K_{barrier/w}$, as the zone of minimum partitioning may account disproportionately for the permeability coefficient.

Solvent physicochemical properties that determine solute partitioning behavior can be analyzed in terms of polarity/polarizability, as usually characterized by the dielectric constant ϵ, and hydrogen-bond donating/accepting capacity (Kamlet et al., 1988; Marcus, 1991). Lipid bilayers are unique in that different regions within the bilayer may possess markedly different solvent properties. The hydrated headgroup region at the bilayer/water interface, for example, resembles a highly polar, hydrogen-bond donating/accepting solvent such as isoamyl alcohol (Diamond & Katz, 1974). The region of ester/ether linkage(s) between the headgroups and the acyl chains is less hydrated but is enriched in hydrogen-bond acceptor groups. The acyl chain region is hydrocarbonlike but its polarizability may be altered by the degree of chain unsaturation and its effective polarity may be increased by its proximity to the hydrated interface.

Whether proximity to the bilayer interface leads to a higher degree of water penetration or interchain hydration (Ho, Slater & Stubbs, 1995) and stronger electrostatic interactions remains unclear. Water penetration was found only in the vicinity of the carbonyl groups in fully hydrated bacterial phospholipid bilayers by X-ray and capacitance measurements (Simon, McIntosh & Latorre, 1982) and in gel and liquid-crystalline phase DPPC bilayers by molecular dynamics simulations (Berger, Edholm & Jahnig, 1997). Very small amounts of water penetration deep into the acyl chain region have been inferred in some ESR and fluorescence experiments (Griffith et al., 1974; Ho et al., 1995) but the influence of the bulky polar spin and fluorescent labels on these measurements is not known. Electrostatic interaction (e.g., the Born and image energies) can arise from the dipoles of the glycerol esters/ethers, the charges in the choline

Table 2. Bulk organic solvent/water partition coefficients for neutral α-substituted *p*-toluic acid analogues at 25°C[a]

Permeant	X	Organic Model Solvents					
		Hexadecane[b]	Hexadecene[b]	Decadiene[b]	Chlorobutane[c]	Butyl ether[c]	Octanol[b]
a	H	$(2.6 \pm 0.0) \times 10^{-1}$	$(5.2 \pm 0.1) \times 10^{-1}$	$(9.0 \pm 0.1) \times 10^{-1}$	3.8 ± 0.4	38 ± 2	230 ± 3
b	Cl	$(1.3 \pm 0.0) \times 10^{-1}$	$(4.2 \pm 0.0) \times 10^{-1}$	$(5.3 \pm 2.4) \times 10^{-1}$	5.0 ± 0.3	58 ± 2	131 ± 9
c	OCH_3	$(3.3 \pm 0.3) \times 10^{-2}$	$(6.4 \pm 0.5) \times 10^{-2}$	$(1.1 \pm 0.1) \times 10^{-1}$	$(6.9 \pm 0.3) \times 10^{-1}$	8.3 ± 0.2	58 ± 2
d	CN	$(2.4 \pm 0.1) \times 10^{-3}$	$(9.6 \pm 1.9\} \times 10^{-3}$	$(1.7 \pm 0.1) \times 10^{-2}$	$(2.0 \pm 0.1) \times 10^{-1}$	1.9 ± 0.0	15.3 ± 0.6
e	OH	$(5.3 \pm 0.2) \times 10^{-5}$	$(2.5 \pm 0.1) \times 10^{-4}$	$(7.3 \pm 0.7) \times 10^{-4}$	$(1.5 \pm 0.1) \times 10^{-3}$	0.25 ± 0.03	8.3 ± 0.2
f	COOH	$(9.3 \pm 0.5) \times 10^{-6}$	$(4.0 \pm 0.2) \times 10^{-5}$	$(1.2 \pm 0.2) \times 10^{-4}$	$(3.2 \pm 0.5) \times 10^{-4}$	0.46 ± 0.03	17.3 ± 0.2
g	$CONH_2$	$(1.5 \pm 0.1) \times 10^{-6}$	$(7.0 \pm 0.6) \times 10^{-6}$	$(4.0 \pm 0.7) \times 10^{-5}$	$(1.1 \pm 0.1) \times 10^{-4}$	0.023 ± 0.00	2.0 ± 0.2

[a] Expressed as mean ± SD.
[b] Determined from previous experiments (Xiang & Anderson, 1994).
[c] This study.

headgroups, and bound water molecules. Previous studies have suggested that bound, organized (i.e., polarized) water molecules at the interface and in the vicinity of the carbonyl groups in the ester linkages are a major contributor to the overall dipole potential or the apparent polarity in the bilayer interior (Flewelling & Hubbell, 1986; Gawrisch et al., 1992; Griffith et al., 1974; Zheng & Vanderkooi, 1992). The electrostatic interaction due to interface dipoles is heterogenous depending on the depth in the bilayer interior (Flewelling & Hubbell, 1986). In the highly ordered mid-chain region of roughly 5–10 Å in length, the dipole potential varies gradually, reaching a maximum in the center of the bilayer. Because of this potential gradient, a neutral but polar molecule may also be subjected to the influence of the hydrated interface. The apparently polar nature of bilayers could also arise from the direct dipole-dipole interaction between polar permeants and methylene groups in lipid acyl chains. These methylene groups possess a small dipole of ca. 0.3 D (Evans & Ulman, 1990) and are capable of creating only a small interface potential of 9 mV/CH_2 (Brockman, 1994). However, in a highly ordered bilayer, these dipoles are highly ordered and in closer contact with permeating solutes.

The above considerations led us to explore in greater detail the apparent solvent characteristics of the barrier domain by comparing functional group contributions obtained from permeability coefficients, thought to reflect primarily changes in $K_{barrier/w}$, with those generated in bulk solvent/water partition coefficient experiments.

Bulk Solvent/Water Partition Coefficients

Six model solvents (hexadecane, hexadecene, decadiene, chlorobutane, butyl ether, and octanol) were chosen to describe, respectively, the possible contributions of polarity, polarizability and hydrogen-bond donating/accepting capacity of the bilayer barrier microenvironment. Hexadecane is nonpolar, resembling the acyl chain region in saturated lipid bilayers. Hexadecene and decadiene have different degrees of chain unsaturation and therefore may be used to describe the possible effects of double bond(s) in egg-PC and cholesterol on barrier properties. Chlorobutane is relatively polar with a dielectric constant of 7.3, which is significantly greater than that of nonpolar hydrocarbons (*ca.* 1.9–2.3). These four solvents have negligible hydrogen-bond donating/accepting capacity. Butyl ether has a single oxygen atom which may function as a hydrogen-bond acceptor resembling those in the ester/ether linkages in DPPC and DHPC bilayers. Octanol, which has the same atomic composition as butyl ether, is capable of both hydrogen-bond donation and acceptance, and is extensively employed as a model solvent for structure-biological activity studies. Bulk solvent/water partition coefficients for the series of *p*-toluic acid analogues in each model solvent system, determined in this or a previous study (Xiang & Anderson, 1994), are presented in Table 2.

The partition coefficients for a series of solutes from water into two different organic solvents, K_1 and K_2, can often be correlated through a linear free energy relationship as described by Eq. 11 (Collander, 1951)

$$\log K_1 = s \log K_2 + i \tag{11}$$

where s and i are constants. The quality of the correlation and the values of the parameters s and i are used to assess similarities in the chemical microenvironments of the two solvent systems. A slope, s, close to one indicates that the two solvents exhibit nearly identical chemical selectivities for the series of solutes under study. An s value of >1 implies that solvent 1 is less polar and therefore more selective to solutes varying in polarity than solvent 2 and vice versa for $s < 1$. As shown in Fig. 8, an excellent correlation ($r = 0.99$) exists between the logarithms of hexadecane/water and chlorobutane/water

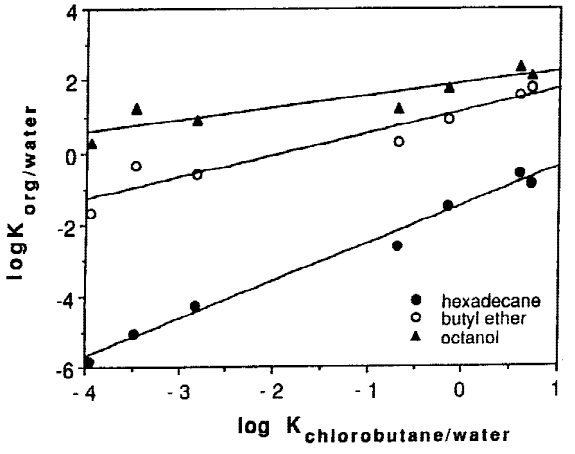

Fig. 8. Linear free energy relationships between various organic solvent (hexadecane, butyl ether, and octanol)/water partition coefficients, $K_{org/w}$, and the chlorobutane/water partition coefficients, $K_{chlorobutane/water}$, of *p*-toluic acid and its α-substituted analogues at 25°C.

partition coefficients with a slope of 1.06, indicating the similar chemical selectivities of these two aprotic non-hydrogen-bonding solvents for the series of *p*-substituted toluic acid analogues. Figure 8 also demonstrates poorer correlations and slopes far from one for the linear free energy relationship when the hydrogen-bond accepting solvent butyl ether or the hydrogen-bond donating/accepting solvent octanol and the non-hydrogen-bonding solvent chlorobutane are compared ($s = 0.60$; $r = 0.96$ for butyl ether and $s = 0.32$; $r = 0.89$ for octanol), using this solute set which contains both hydrogen-bond donating and accepting substituents.

Solvent Nature of the Transport Barrier Microenvironment

The location of the barrier domain and the relative affinities of solute molecules for this domain are unknown *a priori.* However, because of the similarity in molecular size (and therefore diffusivity) among the series of *p*-toluic acid analogues, one can define a linear free energy relationship correlating the logarithms of lipid bilayer permeability coefficients, P_m, with the logarithms of bulk organic solvent-water partition coefficients, $K_{org/w}$:

$$logP_m = slogK_{org/w} + i \qquad (12)$$

As in Eq. 11, the slope, *s*, often referred to as the selectivity coefficient (Katz, Hoffman & Blumenthal, 1983), measures the relative chemical affinities of a series of solutes for the barrier domain in the bilayer versus the organic solvent chosen for the correlation. The most

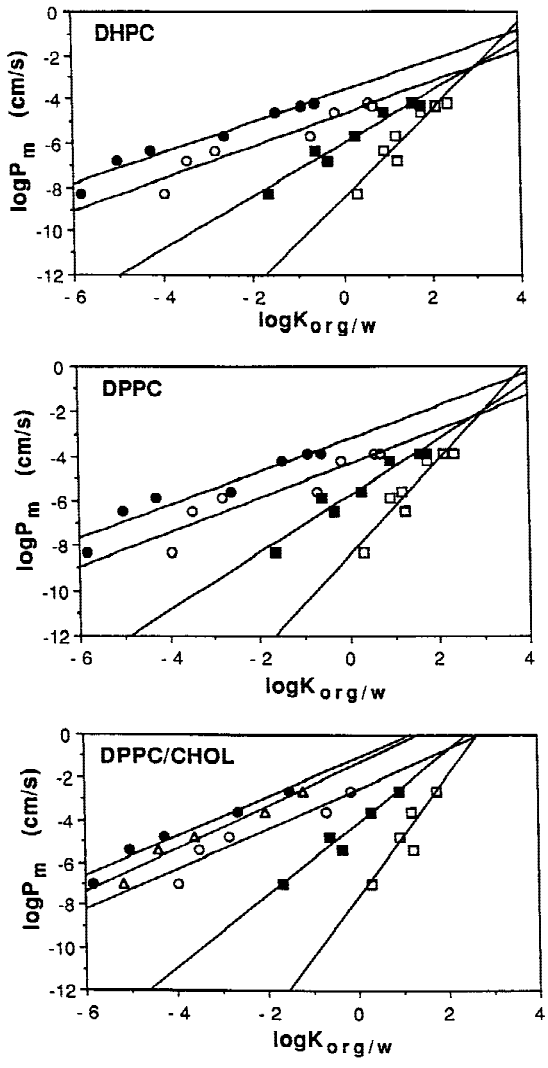

Fig. 9. Linear free energy relationships between the permeability coefficients, P_m, and various model solvent/water partition coefficients, $K_{org/w}$, for *p*-toluic acid and its α-substituted analogues. Key: (●), hexadecane; (○), chlorobutane; (■), butyl ether; (□), octanol; and (△), hexadecene.

suitable model solvent for mimicking the barrier domain is one which provides an *s* value of one, indicating that the chemical selectivity of the barrier domain exactly matches that of the bulk solvent.

Figure 9*A–C* show correlations between log P_m for the neutral species of *p*-toluic acid and its α-substituted analogues across DPPC, DHPC and DPPC/CHOL bilayers, respectively, and log $K_{org/w}$ using various organic solvents (octanol, butyl ether, chlorobutane, decadiene, hexadecene, and hexadecane). The parameter values generated from regression analyses are summarized in Table 3 along with the data for egg-PC bilayers obtained previously using the BLM transport method (Xiang & Anderson, 1994). Correlations of permeabilities in

Table 3. Parameter values generated from linear regression analyses of log-log plots correlating lipid bilayer permeability coefficients and bulk solvent/water partition coefficients according to Eq. 12

Bilayer	Solvent	s	i	Correlation coef.
DHPC	Hexadecane	0.70 ± 0.07	−3.7 ± 0.2	0.978
	Chlorobutane	0.73 ± 0.10	−4.7 ± 0.2	0.958
	Butyl Ether	1.19 ± 0.12	−6.1 ± 0.1	0.977
	Octanol	2.00 ± 0.30	−8.6 ± 0.5	0.950
DPPC	Hexadecane	0.74 ± 0.10	−3.3 ± 0.4	0.955
	Chlorobutane	0.77 ± 0.14	−4.4 ± 0.3	0.928
	Butyl Ether	1.27 ± 0.15	−5.8 ± 0.2	0.965
	Octanol	2.14 ± 0.33	−8.5 ± 0.5	0.945
DPPC/CHOL	Hexadecane	0.93 ± 0.11	−1.10 ± 0.5	0.980
	Hexadecene	1.00 ± 0.11	−1.4 ± 0.4	0.982
	Decadiene	1.13 ± 0.16	−1.5 ± 0.5	0.973
	Chlorobutane	0.95 ± 0.17	−2.6 ± 0.5	0.955
	Butyl Ether	1.70 ± 0.23	−4.2 ± 0.2	0.973
	Octanol	2.84 ± 0.80	−7.8 ± 0.9	0.901
Egg-PC[a]	Hexadecane	0.85 ± 0.03	−0.64 ± 0.11	0.997
	Hexadecene	0.91 ± 0.04	−0.34 ± 0.11	0.996
	Decadiene	0.99 ± 0.04	−0.17 ± 0.12	0.996
	Chlorobutane	0.90 ± 0.04	−0.61 ± 0.11	0.989
	Butyl Ether	1.39 ± 0.19	−2.3 ± 0.2	0.956
	Octanol	2.4 ± 0.5	−5.1 ± 0.7	0.909

[a] Determined from previous experiments using the BLM transport method (Xiang & Anderson, 1994).

DPPC and DHPC bilayers with hexadecene/water and decadiene/water partition coefficients were excluded because, unlike cholesterol and egg-PC, which possess one or more double bonds, the acyl chains in DPPC and DHPC are fully saturated. Although the correlation coefficient is generally higher when the chemical selectivity coefficient (i.e., the slope *s*) is closer to one, it is the value of *s* itself which is both more sensitive to the choice of a model solvent and a more revealing indicator of barrier domain properties. Octanol, a relatively polar, hydrogen-bonding solvent, yields slopes (2.0–2.8) considerably larger than one for all bilayers explored, indicating that the bilayer barrier domains more closely resemble an aprotic hydrocarbon solvent than octanol. This observation indicates that, regardless of chemical composition and phase structure, the barrier domains do not reside in the hydrated interface headgroup regions. Similarly, a transient water-pore pathway cannot be a significant transport route for these permeants. This result contrasts sharply with the alcohol-like polarity profiles across phospholipid bilayers (even at the membrane center) reported by Subczynski et al. (1994). Possibly, their use of polar spin labels (nitroxides) at various positions in the lipid chains to probe the local hydrophobicity may have induced artificially high water concentrations in the vicinity of the spin probes. The extremely low temperature (−150°C) used in the ESR studies may also have contributed to the differences between their results and those obtained in this study.

Even though the barrier microenvironments in DPPC, DHPC, DPPC/CHOL, and egg-PC bilayers are all much less polar than octanol, there are significant differences noted in Table 3. For example, liquid-crystalline bilayers (DPPC/CHOL and egg-PC) exhibit barrier properties most closely matched by partially unsaturated hydrocarbon bulk solvents (e.g., hexadecene or decadiene) whereas the chemical selectivities of the gel-phase bilayers (DHPC and DPPC) are intermediate between those in hexadecane and butyl ether. Thus, slopes significantly less than one (i.e., 0.7) were found in log-log plots of permeability coefficients in gel-phase DPPC and DHPC bilayers against hexadecane/water partition coefficients, while correlations with butyl ether/water partition coefficients yielded slopes of 1.3 and 1.2, respectively. Considered in isolation, this difference could perhaps be ascribed to the relative polarities of hexadecane and butyl ether, which have dipole moments of 0.0 and 1.8 debye units, respectively, but correlations with hexadecane/water and chlorobutane/water partition coefficients are nearly parallel despite the much higher dipole monent of chlorobutane (2.1 debye units). Thus, the differences do not appear to involve polarity. Rather the barrier domains in the gel-phase phospholipid bilayers appear to possess some degree of hydrogen-bond accepting capacity. This may indicate that the ester/ether linkages between the headgroups and the acyl chains reside partially within the barrier domain. In principle, the nonpolar acyl chain region would impose the highest energetic barrier to the transport of polar permeants due to the absence of favorable electrostatic interactions. However, lipid chain ordering within bilayers contributes an additional diffusional resistance and an unfavorable en-

tropic contribution to solute partitioning such that the more rigidly packed peripheral chain region imposes a higher barrier to permeation (Bassolino-Klimas et al., 1993; Marqusee & Dill, 1986; Xiang & Anderson, 1995*b*). Furthermore, a recent molecular dynamics simulation by Marrink and Berendsen (1994) revealed a substantial lowering of water's diffusivity in the headgroup/glycerol linkage region as a result of its hydrogen bonding to these polar groups. The evidence that hydrogen accepting groups lie within the barrier domain in gel-phase bilayers suggests that as bilayers become more ordered, the barrier domain shifts toward the outer portion of the ordered chain region. Since the region of the bilayer in which the ester/ether linkages are localized has a higher density of hydrogen-bonding sites than that found in bulk butyl ether, it is likely that the barrier domain is not limited to the region of the ester/ether linkages but rather extends deeper into the highly ordered chain region within the bilayer interior.

Contrary to the barrier domains in gel-phase phospholipid bilayers, those in more disordered liquid-crystalline bilayers such as DPPC/CHOL or egg-PC exhibit properties resembling slightly polarizable, nonhydrogen accepting hydrocarbons (e.g., hexadecene or decadiene). The slope of a log-log plot of the permeability coefficients in DPPC/CHOL bilayers versus the hexadecene/water partition coefficients is 1.00, while correlations with the hydrogen-bonding solvents (butyl ether and octanol) give slopes substantially greater than one ($s = 1.7$ and 2.8, respectively). Intercalation of 50 mol% cholesterol into gel-phase DPPC bilayers disorders the bilayer chains resulting in a phase-transition to the liquid crystalline state and abolishes the hydrogen-bond acceptor character of the transport barrier domain. Though some evidence suggests that cholesterol interacts with the phospholipid ester groups, it is more likely that the disordering effects of cholesterol in gel-phase DPPC bilayers as demonstrated by the ^{2}H-NMR spectral line shape showing axially symmetric reorientation (Vist & Davis, 1990) cause the barrier domain to be shifted to the deeper acyl chain region where the hydrophobic barrier is higher due to the lack of hydrogen-bonding sites and less favorable electrostatic interactions. This is further supported by the results in egg-PC bilayers which are liquid-crystalline at 25°C even though they contain no cholesterol (Xiang & Anderson, 1994). As shown in Table 3, the barrier domain in egg-PC bilayers resembles decadiene, a nonhydrogen-bonding solvent ($s = 0.99$) which is slightly more polarizable than hexadecane. Possibly the apparently higher polarizabilities observed in both DPPC/CHOL and egg-PC bilayers reflect the presence of a double bond in cholesterol and the presence of an average of one double bond per acyl chain in egg-PC lipids (Fettiplace, Andrews & Haydon, 1971).

Subtle changes in the transport barrier microenvironment have a profound effect on transport of hydrophilic compounds. For example, whereas the ratio of the permeability coefficients for *p*-toluic acid in egg-PC *vs.* DPPC bilayers at 25°C is 8.5×10^3, this ratio for the stronger hydrogen-bond donor α-carboxy-*p*-toluic acid is only 530. The presence of 50 mol% cholesterol in DPPC bilayers, which fluidizes the membrane but also diminishes the hydrogen-bond accepting nature of the barrier domain, has an overall modest effect on the permeability coefficients of hydrogen-bond donating permeants because of the cancellation of these two opposing effects. Glucose, for example, has a van der Waals volume (139 Å^3) comparable with those for the series of *p*-toluic analogues (125–157 Å^3) as estimated from an atomic increment method (Edward, 1970), but the ratio of permeability coefficients for glucose across liquid-crystalline DPPC/CHOL and gel-phase DPPC bilayers is only 2.2 as compared to ratios ranging from 30–100 for the series of *p*-toluic acid analogues.

Because the α-substituents in the series of *p*-toluic acid analogues are well isolated from other functional groups on the same molecule, it is appropriate to assume that the contributions of these substituents to solute permeation are independent properties of the substituents. Functional group contributions to the standard free energy of transfer from water to an organic solvent can be calculated by the equation

$$\Delta(\Delta G^o)_X = -RTln(K_{RX}/K_{RH}) \quad (13)$$

where K_{RX} and K_{RH} are the partition coefficients for the substituted and unsubstituted solutes, respectively. Likewise, because of the similar molecular size and thereby similar diffusivities of the *p*-toluic acid analogues, functional group contributions to the standard free energy of transfer from water to the lipid bilayer barrier domain may be estimated from the permeability coefficients of substituted and unsubstituted permeants, P_{RX} and P_{RH}, respectively, by the equation

$$\Delta(\Delta G^o)_X = -RTln(P_{RX}/P_{RH}) \quad (14)$$

The incremental free energies of transfer for various substituents at the α-position of *p*-toluic acid into the barrier regions of gel-phase DPPC and DHPC bilayers and liquid-crystalline DPPC/CHOL and egg-PC bilayers (the latter of which were obtained previously (Xiang & Anderson, 1994)) are summarized in Table 4 along with those for transfer of the same substituents from water to six organic solvents (octanol, butyl ether, chlorobutane, decadiene, hexadecene, and hexadecane). The incremental free energies of transfer into DPPC/CHOL bilayers are based on an estimated permeability coefficient for *p*-toluic acid, which was too high to measure using the present method. The estimate was obtained from a linear extrapolation of the correlation between log P_m and log $K_{org/w}$ using hexadecene as the optimal organic solvent (*s*

Table 4. Functional group contributions to the free energy (cal/mol) of transfer of *p*-toluic acid and its α-substituted analogues from water into various bilayer barrier domains and model bulk solvents at 25°C[a]

X	DHPC	DPPC	DPPC/CHOL	Egg-PC	Hexadecane	Hexadecene	Decadiene	Chlorobutane	Butyl Ether	Octanol
H	0	0	0	0	0	0	0	0	0	0
Cl	146	0	−	325	409	126	314	−165	−250	350
OCH_3	530	460	1270[b]	687	1240	1260	1240	1010	900	840
CN	2020	2290	2610[b]	2170	2820	2400	2350	1750	1770	1640
OH	2930	2650	4340[b]	3860	5100	4590	4210	4640	2980	2000
COOH	3540	3520	5080[b]	5170	6140	5680	5270	5540	2610	1560
$CONH_2$	5590	6050	7240[b]	6060	7250	6730	6010	6190	4390	2870

[a] Calculated according to Eqs. 13 and 14.
[b] P_m for *p*-toluic acid was estimated from a linear extrapolation of the correlation line between log P_m and log $K_{hexadecene/water}$ (Fig. 9*C*.)

= 1.00). In general, the group contribution data agree with the findings in Fig. 9*A–C* that the barrier domains in gel-phase DPPC and DHPC bilayers resemble a solvent with some hydrogen-bond accepting capacity which is eliminated when a phase transition is induced by intercalation of 50 mol% cholesterol.

Although others have speculated that nonpolar hydrocarbons may be a better choice than octanol as model solvents for the permeability barriers in lipid bilayers, selectivity constants reported previously have been quite close to one for both octanol and nonpolar solvents (Orbach & Finkelstein, 1980; Walter & Gutknecht, 1986). Indeed, Orbach and Finkelstein (1980) have argued that the choice of model solvent is not important because the selectivity constant is nearly the same for all the model solvents employed. However, as pointed out by Walter and Gutknecht (1986), nonpolar and polar, hydrogen bonding solvents often appear to give similar selectivity constants in correlations between permeability coefficients and partitioning data because permeant hydrophilicity is usually varied by changing the number of nonpolar -CH_2-groups. Each -CH_2-group induces only a modest change in the transfer free energy (*ca.* 800 cal/mol) in contrast to free energy changes of 2000–6000 cal/mol induced by polar, hydrogen bonding substituents such as -CN, -OH, -COOH, and -$CONH_2$. Moreover, the methylene group contribution is not highly sensitive to the nature of the organic solvent employed in partitioning studies.

In summary, a vesicular transport method has been developed to measure permeability coefficients of solutes across lipid bilayers. The short time interval (<3 min) for sampling enables measurements of relatively rapid transport processes and the use of HPLC for permeant concentration analyses eliminates the confounding effects of impurities on the measurement of transport fluxes (which may be a very severe and formidable problem for transport using radiolabeled permeants). This study clearly demonstrates that changes in bilayer phase structure alter the location and hydrophobicity of the transport barrier domain. In gel-phase interdigitated and noninterdigitated phospholipid bilayers, the transport barrier domains possess a certain degree of hydrogen-bond accepting capacity. This is consistent with the notion that increasing lipid chain ordering shifts the barrier domain from the ordered hydrocarbon chain interior toward the peripheral region in which the ester/ether linkages between headgroups and acyl chains are localized. Since biological membranes may exist in a gel-phase, a liquid-crystalline phase, or a state of multiphase coexistence, the finding that the barrier microenvironment changes with bilayer phase structure may provide insight into the molecular origins of structure-activity relationships which reflect at least in part a transport component.

This work was supported by a grant from the National Institutes of Health (RO1 GM51347).

References

Anderson, B.D., Higuchi, W.I., Raykar, P.V. 1988. Heterogeneity effects on permeability-partition coefficient relationships in human stratum corneum. *Pharm. Res.* **5:**566–573

Anderson, B.D., Raykar, P.V. 1989. Solute structure-permeability relationships in human stratum corneum. *J. Invest. Dermatol.* **93:** 280–286

Bartlett, G.R. 1959. Phosphorous assay in column chromatography. *J. Biol. Chem.* **234:**466–468

Bassolino-Klimas, D., Alper, H.E., Stouch, T.R. 1993. Solute diffusion in lipid bilayer membranes: An atomic level study by molecular dynamics simulation. *Biochemistry* **32:**12624–12637

Berger, O., Edholm, O., Jahnig, F. 1997. Molecular dynamics simulations of a fluid bilayer of dipalmitoylphosphatidylcholine at full hydration, constant pressure, and constant temperature. *Biophys. J.* **72:**2002–2013

Braganza, L.F., Worcester, D.L. 1986. Hydrostatic pressure induces hydrocarbon chain interdigitation in single-component phospholipid bilayers. *Biochemistry* **25:**2591–2596

Brockman, H. 1994. Dipole potentials of lipid membranes. *Chem. Phys. Lipids* **73:**57–79

Brunner, J., Graham, D.E., Hauser, H., Semenza, G. 1980. Ion and sugar permeabilities of lecithin bilayers: comparison of curved and planar bilayers. *J. Membrane Biol.* **57:**133–141

Cevc, G., Seddon, J.M., Harttung, R., Eggert, W. 1988. Phosphatidylcholine-fatty acid membranes. I. Effects of protonation, salt concentration, temperature and chain length on the colloidal and phase properties of mixed vesicles, bilayers and nonlamellar structures. *Biochim. Biophys. Acta* **940:**219–240

Clowes, A.W., Cherry, R.J., Chapman, D. 1971. Physical properties of lecithin-cerebroside bilayers. *Biochim. Biophys. Acta* **249:**301–317

Collander, R. 1951. The partition of organic compounds between higher alcohols and water. *Acta Chem. Scand.* **5:**774

Diamond, J.M., Katz, Y. 1974. Interpretation of nonelectrolyte partition coefficients between dimyristoyl lecithin and water. *J. Membrane Biol.* **17:**121–154

Diamond, J.M., Szabo, G., Katz, Y. 1974. Theory of nonelectrolyte permeation in a generalized membrane. *J. Membrane Biol.* **17:**148–152

Edward, J.T. 1970. Molecular volumes and the Stokes-Einstein equation. *J. Chem. Ed.* **47:**261–270

Evans, S.D., Ulman, A. 1990. Surface potential studies of alkyl-thiol monolayers adsorbed on gold. *Chem. Phys. Letters* **170:**462–466

Fettiplace, R., Andrews, D.M., Haydon, D.A. 1971. The thickness, composition and structure of some lipid bilayers and natural membranes. *J. Membrane Biol.* **5:**277–296

Flewelling, R.F., Hubbell, W.L. 1986. The membrane dipole potential in a total membrane potential model. *Biophys. J.* **49:**541–552

Gawrisch, K., Ruston, D., Zimmerberg, J., Parsegian, V.A., Rand, R.P., Fuller, N. 1992. Membrane dipole potentials, hydration forces, and the ordering of water at membrane surfaces. *Biophys. J.* **61:**1213–1223

Griffith, O.H., Dehlinger, P.J., Van, S.P. 1974. Shape of the hydrophobic barrier of phospholipid bilayers (evidence for water penetration in biological membranes). *J. Membrane Biol.* **15:**159–192

Ho, C., Slater, S.J., Stubbs, C.D. 1995. Hydration and order in lipid bilayers. *Biochemistry* **34:**6188–6195

Hope, M.J., Bally, M.B., Webb, G., Cullis, P.R. 1985. Production of large unilamellar vesicles by a rapid extrusion procedure. Characterization of size distribution, trapped volume and ability to maintain a membrane potential. *Biochim. Biophys. Acta* **812:**55–65

Huang, T.-H., Lee, C.W.B., Das Gupta, S.K., Blume, A., Griffin, R.G. 1993. A ^{13}C and ^{2}H nuclear magnetic resonance study of phosphatidylcholine/cholesterol interactions: Characterization of liquid-gel phases. *Biochemistry* **32:**13277–13287

Kamlet, M.J., Doherty, R.M., Abraham, M.H., Marcus, Y., Taft, R.W. 1988. Linear solvation energy relationships. 46. An improved equation for correlation and prediction of octanol/water partition coefficients of organic nonelectrolytes (including strong hydrogen bond donor solutes). *J. Phys. Chem.* **92:**5244–5255

Katz, Y., Hoffman, M.E., Blumenthal, R. 1983. Parametric analysis of membrane characteristics and membrane structure. *J. Theor. Biol.* **105:**493–510

Lampe, M.A., Williams, M.L., Elias, P.M. 1983. Human epidermal lipids: characterization and modulations during differentiation. *J. Lipid Res.* **24:**131–140

Leo, A., Hansch, C., Elkins, D. 1971. Partition coefficients and their uses. *Chem. Rev.* **71:**525–616

Levin, V.A. 1980. Relationship of octanol/water partition coefficient and molecular weight to rat brain capillary permeability. *J. Med. Chem.* **23:**682–684

Marcus, Y. 1991. Linear solvation energy relationships. Correlation and prediction of the distribution of organic solutes between water and immiscible organic solvents. *J. Phys. Chem.* **95:**8886–8891

Marqusee, J.A., Dill, K.A. 1986. Solute partitioning into chain molecule interphases: Monolayers, bilayer membranes, and micelles. *J. Chem. Phys.* **85:**434–444

Marra-Feil, M. 1995. Lipid phase structure contributions to bilayer barrier function. Ph.D. Thesis, University of Utah

Marrink, S.J., Berendsen, H.J.C. 1994. Simulation of water transport through a lipid membrane. *J. Phys. Chem.* **98:**4155–4168

Orbach, E., Finkelstein, A. 1980. The nonelectrolyte permeability of planar lipid bilayer membranes. *J. Gen. Physiol.* **75:**427–436

Overton, E. 1899. Ueber die allgemeinen osmotischen Eigenschaften der Zelle, ihre vermutlichen Ursachen und ihre Bedeutung fur die Physiologie. *Vjschr. Naturforsch. Ges. Zurich* **44:**88

Rapoport, S.I., Ohno, K., Pettigrew, K.D. 1979. Drug entry into the brain. *Brain Research* **172:**354–359

Ruocco, M.J., Siminovitch, D.J., Griffin, R.G. 1985. Comparative study of the gel phases of ether- and ester-linked phosphatidylcholines. *Biochemistry* **24:**2406–2411

Sankaram, M.B., Thompson, T.E. 1991. Cholesterol-induced fluid-phase immiscibility in membranes. *Proc. Natl. Acad. Sci. USA* **88:**8686–8690

Simon, S.A., McIntosh, T.J., Latorre, R. 1982. Influence of cholesterol on water penetration into bilayers. *Science* **216:**65–66

Singer, S.J., Nicolson, G.L. 1972. The fluid mosaic model of the structure of cell membranes. *Science* **175:**720–731

Snyder, F. 1985. Metabolism, Regulation, and Function of Ether-Linked Glycerolipids. *In:* Biochemistry of Lipids and Membranes. D.E. Vance and J.E. Vance, editors. pp. 271–298. Benjamin/Cummings, Menlo Park, CA

Subczynski, W.K., Wisniewska, A., Yin, J.-J., Hyde, J.S., Kusumi, A. 1994. Hydrophobic barriers of lipid bilayer membranes formed by reduction of water penetration by alkyl chain unsaturation and cholesterol. *Biochemistry* **33:**7670–7681

van Blitterswijk, W.J., van der Meer, B.W., Hilkmann, H. 1987. Quantitative contributions of cholesterol and the individual classes of phospholipids and their degree of fatty acyl (un)saturation to membrane fluidity measured by fluorescence polarization. *Biochemistry* **26:**1746–1756

Vist, M.R., Davis, J.H. 1990. Phase equilibria of cholesterol/dipalmitoylphosphatidylcholine mixtures: ^{2}H nuclear magnetic resonance and differential scanning calorimetry. *Biochemistry* **29:**451–464

Walter, A., Gutknecht, J. 1986. Permeability of small nonelectrolytes through lipid bilayer membranes. *J. Membrane Biol.* **90:**207–217

White, S.H., Mirejovsky, D., King, G.I. 1988. Structure of lamellar lipid domains and corneocyte envelopes of murine stratum corneum. An X-ray diffraction study. *Biochemistry* **27:**3725–3732

Xiang, T.-X., Anderson, B.D. 1994. Substituent contributions to the permeability of substituted *p*-toluic acids in lipid bilayer membranes. *J. Pharm. Sci.* **83:**1511–1518

Xiang, T.-X., Anderson, B.D. 1995*a.* Mean molecular potentials in a model lipid bilayer: A molecular dynamics simulation. *J. Chem. Phys.* **103:**8666–8678

Xiang, T.-X., Anderson, B.D. 1995*b*. Phospholipid surface density determines the partitioning and permeability of acetic acid in DMPC: cholesterol bilayers. *J. Membrane Biol.* **148:**157–167

Xiang, T.-X., Anderson, B.D. 1997. Permeability of acetic acid across gel and liquid-crystalline lipid bilayers conforms to free-surface-area theory. *Biophys. J.* **72:**223–237

Xiang, T.-X., Anderson, B.D. 1998. Phase structures of binary lipid bilayers as revealed by permeability of small molecules. *Biochim. Biophys. Acta* **1370:** 64–76

Xiang, T.-X., Chen, X., Anderson, B.D. 1992. Transport methods for probing the barrier domain of lipid bilayer membranes. *Biophys. J.* **63:**78–88

Zheng, C., Vanderkooi, G. 1992. Molecular origin of the internal dipole potential in lipid bilayers: calculation of the electrostatic potential. *Biophys. J.* **63:**935–941